International Journal of Multidisciplinary and Current Research ISSN: 2321-3124
Research Article Available at: http://ijmcr.com

QPRM calculation of Band Structures in A~100

O. Jdair[#], J. Inchaouh[#], M. K. Jammari[^], A. Khouaja[#], M. Ferricha-Alami[#] and H. Chakir[#]

[#]Department of Physics, LPMC-ERSA, Faculty of Sciences Ben M'Sik Hassan II Casablanca University, Casablanca, Morocco B.P. 5366
[^]Department of Physics, LPN , Faculty of Sciences Ain chock, Hassan II Casablanca University, Casablanca, Morocco B.P. 5366

Accepted 15 May 2017, Available online 31 May 2017, **Vol.5 (May/June 2017 issue)**

Abstract

Study of nuclear structure exhibits a wide variety of modes of nuclear excitations. The A ~ 100 mass region demonstrate a rich diversity of structure phenomena. In this context we utilized the theoretical method based on the quasiparticle-phonon coupling is developed for a microscopic description of the low-lying states for odd nuclei of the A ~ 100 mass of transitional region with application to Sr, Zr, Mo and Ru. The individual excitation is retained in a deformed average field of Nilsson and a monopole pairing interaction. The collectif vibrational motion is represented by including the quadrupole phonon term given from the Tamm-Dancoff Approximation. The two effects of recoil and Coriolis forces are included with the assumption of a symmetric rotation motion. To determine the intrinsic states of an odd-nucleus we adopted an exact diagonalization in the basis of both 1-quasiparticle and quasiparticle-phonon states. This contribution will conclude with an overview of recent results obtained for theoretical level schemes of ^{99}Sr, ^{101}Zr, ^{103}Mo and ^{105}Ru and compared with the existing experimental data.

Keywords: *The A ~ 100 mass region, BCS approximation, Low-lying levels, TDA phonon*

1. Introduction

The properties of the low lying states near A ~ 100 are particularly fascinating to study several interesting features of nuclear structure in this mass region. There has been much study of the quasi-collectivity in these nuclei and its evolution with spins and neutron numbers. For the even 38Sr and $_{40}$Zr isotopes a sudden onset of strong deformation is observed from N = 60, whereas the lighter isotopes up to N=58 are rather spherical. However, the abrupt change of the deformation quickly washes out when moving away from Z = 38. There were showed for N=59 isotones, using the quasiparticle-Rotor-Model, that some shapes coexist, particularly the two unique-parity states $\pi g_{9/2}$ and $\nu h_{11/2}$, in the structure of ^{97}Sr, ^{99}Zr and ^{96}Rb isotopes [1, 2]. The clear identification of the bandhead spins, their deformations and the Nilsson orbitals of N=59 isotones, has given a new insights in understanding the mechanisms responsible of this rapid change in shapes, which are highlighted from the quadrupole moment measurements of the ground state for Rubidium isotopes [2]. However, using the self-consistent Total Routhian Surface (TRS) model for N > 59 isotones, there have been found that the nuclear structure of ^{105}Mo and ^{103}Zr has a medium triaxiality parameter of γ = -19° and γ = 0° [3], respectively.

*Corresponding author's ORCID ID: 0000-0000-0000-0000
DOI: https://doi.org/10.14741/ijmcr.v.5.3.19

The triaxial effect, sign of strong deformation, is more important for Mo isotopes than Zr ones, using RTRP and TRS models [3, 4]. Experimentally, producing Zr and Mo isotopes from ^{238}U(α,f) fusion-fission reaction mechanism, the analysis of experimental data performed in the framework of the particle–rotor-model showed that the triaxial degree of freedom is more important for Mo than Zr isotopes [5]. In these calculations, the Cranked shell model was used for the study of the crossing frequency of the aligned band. It was concluded that the alignment of $\nu h_{11/2}$ neutron orbital is responsible for the first band crossing in the even Zr and Mo isotopes [5], which has a great consequence on the behavior of $5/2^-(532)$ bands in the odd Zr and Mo isotopes. It would be interesting to see if these results remain valid for neighboring nuclei Sr and Ru.

In the transitional region A ~ 100, the nuclear shape is soft spherical-deformed, which is theoretically a reason to do not use a rigid triaxiality. It is then a better way to treat this spherical-deformed shape by using the coupling between (axial) rotation and vibration. Therefore, in our work, we have used a Soloviev [6] inspired model: Quasiparticle Phonon plus rotor (QPRM), where TDA phonon was used instead of RPA one. We have developed a microscopic description for the low-lying excited states of odd-A = 99 and 105 nuclei [7-8]. For the transitional region, a microscopic structure is considered for the quadrupole phonon by means of Tamm-Dancoff

Approximation (TDA), developed in the Ring-Schuk book [9]. This method is microscopic and provides two-quasiparticle structure of the quadrupole vibrational core (γ-phonon) in contrast to the phenomenological model in which the phonon structure is excluded. The article is presented in two main parts. First, we present advances in the understanding of QPRM Method. Second we present the results, briefly describe the QPRM method that we have used to perform our systematic tests, discuss the results obtained in comparison to the experimental data from [10, 11, 12, 13] for neutron-rich Sr, Zr, Mo and Ru isotopes, and, finally, present the conclusions.

2. Theoretical Procedures

The current release of the QPRM code, which is used for the transitional region A~ 100 with particular investigation of the low-lying states of ^{99}Sr, ^{101}Zr, ^{103}Mo and ^{105}Ru which are treated as a system of even-even core plus an extra nucleon. We take in consideration the following steps: Nilsson, BCS and TDA calculations. We make a brief reminder of the quasiparticle-phonon coupling plus rotor method (QPRM) developed in [7, 8]. The excited state for an odd-nucleus are then reproduced has been combinaison of rotational state.

$$\left|\mathrm{I}_\alpha\right\rangle=\sum_{\mathrm{K}}\mathrm{b}_{\mathrm{K}}^{\mathrm{I}_\alpha}\left|\mathrm{k}\right\rangle \tag{1}$$

The index α labels the states with the same angular momentum and b_K^I represents the amplitudes of Coriolis mixing determined after diagonalization of the total Hamiltonien which is separated into three terms: the intrinsic Hamiltonian H_{int}, the rotational terms H_I, and the Coriolis force H_C [14].

$H = H_{int} + H_I + H_C$

Where

$H_I = A_R(I^2 - I_3^2)$ (2-a)

$H_C = -A_R(I_+J_- + I_-J_+)$ (2-b)

With $I_\pm = I_1 \pm iI_2$, $J_\pm = J_1 \pm iJ_2$ and the rotational coefficient $A_R = \hbar^2/2\Im$. The intrinsic motion is essentially represented by a quasiparticle system (BCS approximation) by considering a Nilsson average deformed field H_{sp} [15] plus a monopole pairing interaction [9]. As residual interaction, the quadrupole-quadrupole interaction H_Q [9] and the recoil force H_J [16] are also added to H_{int}.

$H_{int} = H_{sp} + H_P + H_Q + H_J$ (3)

Where

$$\mathrm{H}_{\mathrm{sp}}=\sum_{\nu\tau}\mathrm{e}_{\nu\tau}\mathrm{a}_{\nu\tau}^{+}\mathrm{a}_{\nu\tau} \tag{3-a}$$

$$\mathrm{H}_{\mathrm{p}}=-\sum_{\nu\mu\tau}\mathrm{G}_{\tau}\mathrm{a}_{\nu\tau}^{+}\mathrm{a}_{-\nu\tau}^{+}\mathrm{a}_{-\mu\tau}\mathrm{a}_{\mu\tau} \tag{3-b}$$

$$\mathrm{H}_{\mathrm{Q}}=-\frac{1}{2}\chi\sum_{\tau\tau'}\{\mathrm{Q}_{22}^{+}(\tau)\mathrm{Q}_{22}(\tau')+\mathrm{Q}_{2-2}^{+}(\tau)\mathrm{Q}_{2-2}(\tau')\} \tag{3-c}$$

$$\mathrm{H}_{\mathrm{J}}=\frac{1}{2}\mathrm{A}_{\mathrm{R}}\sum_{\tau\tau'}(\mathrm{J}_{+}(\tau)\mathrm{J}_{-}(\tau')+\mathrm{J}_{-}(\tau)\mathrm{J}_{+}(\tau')) \tag{3-d}$$

Where $a^+_{\nu\tau}$ ($a_{\nu\tau}$) is the operator that creates (destroys) a particle of nucleon type τ (neutron or proton) in a Nilsson orbital and with an energy $e_{\nu\tau}$. The quantum number ν stands for the asymptotic quantum along numbers [N, n_z, Λ] with the projection Ω_ν of the particle angular momentum along the symmetry axis. The quadrupole moment of mass with γ = ±2 is given as one-body interaction

$$\mathrm{Q}_{2\gamma}(\tau)=\sum_{\nu\tau\mu}\left\langle\nu\tau\left|\mathrm{r}^2\mathrm{Y}_{2\gamma}\right|\mu\tau\right\rangle\mathrm{a}_{\nu\tau}^{+}\mathrm{a}_{\mu\tau} \tag{4}$$

Diagonalzation of the total Hamiltonian is performed under basis formed by symmetrised rotational functions [16].

$$\left|\mathrm{IMK}\rho\right\rangle=\sqrt{\frac{2\mathrm{I}+1}{16\pi^2}}\left\{\mathrm{D}_{\mathrm{MK}}^{\mathrm{I}}\left|\mathrm{K}\rho\right\rangle+(-)^{\mathrm{I}+\mathrm{K}}\mathrm{D}_{\mathrm{M}-\mathrm{K}}^{\mathrm{I}}\left|\overline{\mathrm{K}\rho}\right\rangle\right\} \tag{5}$$

Here ρ is the quantum number of a given intrinsic states with a projection K of the intrinsic angular momentum along the symmetry axis. $|K_\rho\rangle$ can be obtained by resolution of the secular problem

$$H_{\mathrm{int}}\left|K_\rho\right\rangle=(H_{sp}+H_P+H_Q+H_J)\left|K_\rho\right\rangle=E_{K_\rho}^{\mathrm{int}}\left|K_\rho\right\rangle \tag{6}$$

As it is well known, D^I_{MK} is the rotational matrix and is an eigenfunction of I^2 and I^3 with respective eigenvalue I(I+1) and K. Thus, a diagonalization of H within the basis states, equation (5) requires essentially to determine the matrix element of the Coriolis term H_C [14]

$$\left\langle\mathrm{IMK}'_{\rho'}\left|\mathrm{H}_{\mathrm{C}}\right|\mathrm{IMK}_{\rho}\right\rangle=-\mathrm{A}_{\mathrm{R}}\left\{(-)^{\mathrm{I}+\frac{1}{2}}\left(\mathrm{I}+\frac{1}{2}\right)\left\langle\mathrm{K}'_{\rho'}\left|\mathrm{J}_{+}\right|\overline{\mathrm{K}\rho}\right\rangle\delta_{\mathrm{K}'\frac{1}{2}}\delta_{\mathrm{K}\frac{1}{2}}+\sqrt{(\mathrm{I}\mp\mathrm{K})(\mathrm{I}\pm\mathrm{K}+1)}\left\langle\mathrm{K}'_{\rho'}\left|\mathrm{J}_{\pm}\right|\mathrm{K}\rho\right\rangle\delta_{\mathrm{K}',\mathrm{K}\pm1}\right\} \tag{7}$$

In the form of the QPRM method, configuration for wave functions of an intrinsic state $\left|K_\rho\right\rangle$ (2) must renferms contributions of both one-quasiparticle and quasiparticle-phonon components.

$$|\mathrm{K}\rangle=\left(\sum_{\nu}\mathrm{C}_{\nu}^{\rho}\delta_{\mathrm{K}\Omega_\nu}\alpha_{\nu\tau}^{+}+\sum_{\nu\gamma}\mathrm{D}_{\nu\gamma}^{\rho}\delta_{\mathrm{K}=\Omega_\nu+\gamma}\alpha_{\nu\tau}^{+}\mathrm{A}_{\gamma}^{+}\right)|\mathrm{BCS}\rangle \tag{8}$$

With $\left|BCS\right\rangle$ is the BCS ground state and $\alpha^+_{\nu\tau}$ represents the creator quasiparticle operator for a nuclear τ. The quadrupole-phonon operator is defined in the frame of the Tamm-Dancoff Approximation (TDA) [9].

$$\mathrm{A}_{\gamma}^{+}=\frac{1}{2}\sum_{\nu\mu\tau}\left(\mathrm{X}_{\gamma}^{\tau}\right)_{\nu\tau}\alpha_{\nu\tau}^{+}\alpha_{\mu\tau}^{+} \tag{9}$$

This expression permits a microscopic structure description for the quadrupole vibrational core (γ-phonon state) by showing the X-amplitudes which are related to two-quasiparticle excitations.

The resolution of (3) for an odd-A nucleus is perfected by a diagonalization within a basis formed by one-quasiparticle states (1-qp) and quasiparticle-phonon coupling states (qp-ph$_\gamma$). If we retain only the terms that do not have a zero matrix element within the states of this basis, the intrinsic Hamiltonian is then reduced to

$$H_{int} = H_{BCS} + H_{11}^{Q} + H_{20}^{Q} + H_{22}^{Q} + H_{31}^{Q} + H_{11}^{J} + H_{20}^{J} + H_{22}^{J} + H_{31}^{J} + H_{22}^{'P} \quad (10)$$

The Q and J terms are related respectively to quadrupole and recoil forces. The last term is $H_{22}^{'P}$ is a residual pairing interaction which was neglected in BCS approximation. The interaction between two-1qp states and qp-Ph$_\gamma$ states are given respectively by L_{11} and L_{22} matrix elements and that between 1-qp and qp-ph$_\gamma$ states by L_{31}. They are written as follows [7, 8].

$$L_{11} = \langle BCS | \alpha_{K'\tau} (H_{BCS} + H_{11}^{Q} + H_{11}^{J}) \alpha_{K\tau}^{+} | BCS \rangle \quad (11)$$

$$L_{22} = \langle BCS | A_{\gamma} \alpha_{K'\tau} (H_{BCS} + H_{11}^{Q} + H_{11}^{J} + H_{22}^{Q} + H_{22}^{J} + H_{22}^{'P}) \alpha_{K\tau}^{+} A_{\gamma}^{+} | BCS \rangle \quad (12)$$

$$L_{31} = \langle BCS | A_{\gamma} \alpha_{K'\tau} (H_{20}^{Q} + H_{20}^{J} + H_{31}^{Q} + H_{31}^{J}) \alpha_{K\tau}^{+} | BCS \rangle \quad (13)$$

The eigenvalue problem is written in matrix form

$$\begin{pmatrix} L_{11} & L_{31} \\ L_{31} & L_{22} \end{pmatrix} \begin{pmatrix} C_K^{\rho} \\ D_{K\gamma}^{\rho} \end{pmatrix} = E_{K_\rho}^{intr} \begin{pmatrix} C_K^{\rho} \\ D_{K_\gamma}^{\rho} \end{pmatrix} \quad (14)$$

Where C_K^{ρ} represents the 1-qp component and $D_{K_\gamma}^{\rho}$ the qp-ph$_\gamma$ component. The intrinsic eigenvalue E_K^{int} corresponds to the eigenvector (8).

3. Results and discussion

In this section, we focus on selected results for several chains of neutron-rich for the transitional region A~100. We base our theoretical analyses on QPRM calculations which are treated as a system of even-even core plus an extra nucleon. We have developed this code in respect to the following steps: Nilsson, BCS and TDA calculations. We have diagonalized the total Hamiltonian taking into account the rotational motion. For the case of Nilsson calculation, we have reproduced the even-even core structure using conjointly the deformation parameter ε_2 from Moller data [17] and from Meyer data [18], the Kappa = 0.068 and Mu = 0.35 parameters of deformed average Nilsson field. The BCS pairing was fixed for proton and neutron by the well-known phenomenological relation $\Delta_p=\Delta_n=12/A^{1/2}$ [19]. And, for TDA calculation, the parameter of quadrupole force χ was fitted from the experimental energy of quadrupole vibrational core using the experimental from [20, 21, 22, 23], where ^{98}Sr, ^{100}Zr, ^{102}Mo and ^{104}Ru have E(2^+) =144 keV, E(2^+) =212keV, E(2^+) =295 keV and E(2^+) =358 keV respectively .The inertia parameters are determined semi-empirically using the energy of first excited state ($\varepsilon_2^2 \approx 1176(A^{7/3}E(2^+))^{-1}$) [24, 25].

The level energy is a function of deformation parameter (ε_2) and the pairing correlation $G_p=19.6A^{-1}$ and $G_n=(19.6\text{-}15.7(N\text{-}Z)A^{-1})A^{-1}$ are obtained phenomenologicaly [26].

For the special case of ^{99} Sr, the core ^{98}Sr is localised with the deformation parameter ε_2 = 0.325 and the shell effect is completely degenerated. We have to primarily identify the ground state from the excited one in a region where the excitation gap is more important regarding the deformation parameter. The result obtained by our Nilsson calculations for ^{98}Sr is presented in table1.

The 3/2+(411) positive parity state (candidate for it is ground state) is calculated with the structure (approximately 92%$g_{7/2}$, 29.5% $d_{5/2}$, 17.5% $d_{3/2}$, 18.7% $g_{9/2}$) which imply the dominance of $g_{7/2}$ orbital and expose the weak Coriolis mixage, whereas for 1/2+(431) (with 65.3%$g_{9/2}$, 64.9% $d_{5/2}$, 25.6% $g_{7/2}$, 28.1% $s_{1/2}$) shows a strong Coriolis mixage. For the negative parity state we perceive the strong Coriolis mixing and a dominance of the $h_{11/2}$ orbital for 5/2$^-$(532). If there is no excitation of core particles, then the valence neutron can take on all neighbouring Nilsson orbits $2d_{5/2}$, $1g_{7/2}$, $3s_{1/2}$, $2d_{3/2}$ and $1h_{11/2}$ with equal probability. Those orbits are undoubtely correlated with one another through Coriolis interaction with the core. Since these orbits tend to be nearly equally spaced as deformation parameter ε_2 approaches to value 0.3, there is no reason why any one of these orbits will not contribute to the band-mixing, therefore we consider all five of them. We introduce the BCS method in which the correlation probability between quasi-particle operators (creation and annihilation) is well determined**.** In table 2, the subsequent excited states, provided by BCS numerically with a precision of 10^{-7} after 7 iterations, are presented for ^{99}Sr. Around the Fermi level, 10 up and down levels, candidates to be a ground state are treated. For each identified level, the energy is calculated and the occupation (U) and vacancy (V) probabilities are determined. From the energy level close to the Fermi one, we could have a confusing decision if we treat and find out the ground state only in its energy level (the closest energy to the Fermi level).

Table 1: Calculated energies and Coriolis-mixing amplitude of intrinsic states in ^{99}Sr near of the Fermi energy

Nilsson orbitals	Energies of each particle (in ħω)	Asymptotic Nilsson components (with corresponding spherical orbitals)				
		[4 0 2](2d$_{3/2}$)	**[4 1 1](1g$_{7/2}$)**	**[4 2 2](2d$_{5/2}$)**	**[4 3 1](1g$_{9/2}$)**	
3/2+(411)	5.714	-0.175	**0.920**	0.295	-0.187	
3/2+(422)	5.433	0.177	-0.241	**0.817**	0.492	
		[4 0 0](2d$_{3/2}$)	**[4 1 1](3s$_{1/2}$)**	**[4 2 0](1g$_{7/2}$)**	**[4 3 1](2d$_{5/2}$)**	**[4 4 0](1g$_{9/2}$)**
1/2+(411)	5.874	-0.173	**0.895**	0.362	-0.163	-0.100
1/2+(420)	5.383	0.197	-0.196	**0.816**	0.464	-0.201
1/2+(431)	5.118	-0.069	0.281	-0.256	0.649	0.653
		[4 0 2](1g$_{7/2}$)	**[4 1 3](2d$_{5/2}$)**	**[4 2 2](1g$_{9/2}$)**		
5/2+(413)	5.782	-0.178	**0.917**	0.355		
5/2+(422)	4.927	0.168	-0.332	**0.927**		
5/2+(402)	6.098	**0.979**	0.158	-0.120		
		[4 0 4](1g$_{7/2}$)		**[4 1 3](1g$_{9/2}$)**		
7/2+(404)	6.124	0.974		0.222		
7/2+(413)	5.240	-0.223		**0.974**		
		[4 0 4](1g$_{9/2}$)				
9/2+(404)	5.557	**1.000**				
		[5 0 3](2f$_{5/2}$)	**[5 1 2](1h$_{9/2}$)**	**[5 2 3](2f$_{7/2}$)**	**[5 3 2](1h$_{11/2}$)**	
5/2-(532)	5.694	-0.060	0.261	-0.386	**0.882**	
		[3 0 1](2p$_{1/2}$)	**[3 1 0](1f$_{5/2}$)**	**[3 2 1](2p$_{3/2}$)**	**[3 3 0](1f$_{7/2}$)**	
1/2-(301)	5.167	**0.956**	0.280	-0.073	-0.045	
		[5 0 3](1h$_{9/2}$)	**[5 1 4](2f$_{7/2}$)**	**[5 2 3](1h$_{11/2}$)**		
7/2-(523)	5.927	0.157	-0.294	**0.942**		
		[3 0 3](1f$_{5/2}$)		**[3 1 2](1f$_{7/2}$)**		
5/2-(303)	5.143	**0.966**		0.255		
		[5 0 5](1h$_{9/2}$)		**[5 1 4](1h$_{11/2}$)**		
9/2-(514)	6.222	-0.206		**0.978**		
		[5 0 1](3p$_{1/2}$)	**[5 1 0](2f$_{5/2}$)**	**[5 2 1](3p$_{1/2}$)**	**[5 3 0](1h$_{9/2}$)**	**[5 4 1](2f$_{7/2}$)**	**[5 5 0](1h$_{11/2}$)**
1/2-(541)	5.924	0.051	-0.058	0.363	0.015	0.620	**0.689**
1/2-(550)	5.389	-0.029	0.112	-0.245	0.468	-0.541	**0.643**
1/2-(530)	6.146	-0.054	0.291	-0.167	**0.717**	0.590	-0.143
		[5 0 1](3p$_{1/2}$)	**[5 1 2](1h$_{9/2}$)**	**[5 2 1](3p$_{1/2}$)**	**[5 3 2](1h$_{11/2}$)**	**[5 4 1](2f$_{7/2}$)**	
3/2-(541)	5.504	0.050	-0.140	0.389	-0.455	**0.786**	

Table 2: Energy of 20 levels of quasi-particle calculated for ^{99}Sr (neutrons case)

Number	Identification	EQP(MEV)	U	V
21	5/2+(422)	6.098004	0.098877	0.995100
22	1/2+(431)	4.772874	0.126732	0.991937
23	5/2-(303)	4.551124	0.133018	0.991114
24	1/2-(301)	4.535018	0.133499	0.991049
25	7/2+(413)	3.709811	0.163952	0.986468
26	1/2+(420)	2.575156	0.240011	0.970770
27	1/2-(550)	2.476344	0.250256	0.968180
28	3/2+(422)	2.128516	0.295017	0.955492
29	3/2-(541)	1.618642	0.405521	0.914086
30	9/2+(404)	1.336147	0.529254	0.848464
		Level of Fermi		
31	3/2+(411)	1.427856	0.878047	0.478574
32	5/2-(532)	1.429102	0.878370	0.477981
33	5/2+(413)	2.004617	0.948956	0.315409
34	1/2+(411)	2.725895	0.974138	0.225955
35	1/2-(541)	3.225543	0.981891	0.189446
36	7/2-(523)	3.239222	0.982051	0.188615
37	5/2+(402)	4.293308	0.989986	0.141166
38	1/2-(530)	5.047481	0.992806	0.119733
39	7/2+(404)	5.202647	0.993236	0.116111
40	1/2+(660)	5.335202	0.993574	0.113188

Table 3: BCS eigen-values for Nilsson orbitals of ^{98}Sr

<μ /	<ν /	$E_\mu + E_\nu$
5/2+(422)	7/2+(413)	9.807815
5/2+(422)	3/2+(422)	8.226520
5/2+(422)	3/2+(411)	7.525860
5/2+(422)	7/2+(404)	11.300651
-1/2+(431)	1/2+(431)	9.545749
-1/2+(431)	1/2+(420)	7.348030
1/2+(431)	3/2+(422)	6.901391
1/2+(431)	3/2+(411)	6.200731
-1/2+(431)	1/2+(411)	7.498769
-1/2+(431)	1/2+(660)	10.108077
5/2-(303)	3/2-(541)	6.169766
5/2-(303)	7/2-(523)	7.790345
-1/2-(301)	1/2-(301)	9.070036
-1/2-(301)	1/2-(550)	7.011362
1/2-(301)	3/2-(541)	6.153660
-1/2-(301)	1/2-(541)	7.760561
-1/2-(301)	1/2-(530)	9.582499
7/2+(413)	9/2+(404)	5.045957
7/2+(413)	5/2+(413)	5.714427
7/2+(413)	5/2+(402)	8.003118
-1/2+(420)	1/2+(420)	5.150312
1/2+(420)	3/2+(422)	4.703672
-1/2+(420)	1/2+(411)	5.301050
1/2+(420)	3/2+(411)	4.003012
-1/2+(420)	1/2+(660)	7.910358
-1/2-(550)	1/2-(550)	4.952687
1/2-(550)	3/2-(541)	4.094986
-1/2-(550)	1/2-(541)	5.701887
-1/2-(550)	1/2-(530)	7.523825
3/2+(422)	5/2+(413)	4.133133
3/2+(422)	1/2+(411)	4.854411
3/2+(422)	5/2+(402)	6.421824
3/2+(422)	1/2+(660)	7.463718
3/2-(541)	**5/2-(532)**	**3.047744**
3/2-(541)	1/2-(541)	4.844185
3/2-(541)	1/2-(530)	6.666123
9/2+(404)	7/2+(404)	6.538793
3/2+(411)	**5/2+(413)**	**3.432473**
3/2+(411)	**1/2+(411)**	**4.153751**

In table 3, we carried out the whole possible ground and excited states correlated from particular states presented in table 2.

The combinations between states (columns 1 and 2) are treated in the approximation of quasiparticle independent model, where the Hamiltonian is:

$$H = U_0 + \sum_{\mu\nu}(E_\mu + E_\nu)\alpha_\mu^+\alpha_\nu$$

and the correspondent energy is presented in column 3. We find out three possible combinations of states. With smallest energy ($E_\mu + E_\nu$) according to the Fermi level, the ground state could be formed from the couple ($3/2^-$[541], $5/2^-$[532]) with energy level of 3.048 MeV, the couple ($3/2^+$[411], $5/2^+$[413]) with 3.432 MeV, or the couple ($3/2^+$[411], $1/2^+$[411]) with 4.153 MeV. Therefore, when comparing these eigen-values with the ones from table 1, we could expect one of the $5/2^+$[413], $5/2^-$[532] and $3/2^+$[411] orbitals to be the ground state of ^{99}Sr.

We refer to figure 1 in order to demonstrate the contribution of each term in the intrinsic Hamiltonian (10) for the energy evolution of intrinsic states (assigned by the dominant one-quasiparticle configuration or Nilsson orbital) and which are positioned near the Fermi level in ^{99}Sr isotope. The dashed lines connect the states marked by their asymptotic quantum number Ω^π [N, n_z, Λ], where N is principle quantum number, n_z is number of nodes of the wave function in the z-direction (the number of times the radial wave function crosses zero). Larger n_z values corresponds to wave function more extended in the z-direction which means lower energy orbits, Λ is the projection of the orbital angular momentum on to the z-axis, and Ω is the quantum number that corresponds to the third component of the angular momentum in the intrinsic frame.

Table 4: Energy (≤1.5 Mev) and structure of intrinsic states in ^{99}Sr

K^{π}	Energy Exp. (keV)	Energy Th. (keV)	1-qp	C_{ν}	qp-Ph$_{\gamma}$	D_{ν}
3/2+	0	0	3/2+(411)	0.836	3/2+(411)	0.836
1/2+	-	37	1/2+(411)	0.694	1/2+(411)	0.694
				0.946	5/2+(413)+Q_{22}	0.726
5/2+	-	345	5/2+(413)	0.825	5/2+(413)	0.825
				0.874	9/2+(404)+Q_{22}	0.962
1/2+	-	585	1/2+(420)	0.694	1/2+(420)	0.694
5/2-	422	626	5/2-(532)	0.943	5/2-(532)	0.943
3/2+	1071	686	3/2+(422)	0.782	3/2+(422)	0.782
9/2+	377	690	9/2+(404)	0.966	9/2+(404)	0.966
3/2-	-	757	3/2-(541)	0.882	3/2-(541)	0.882

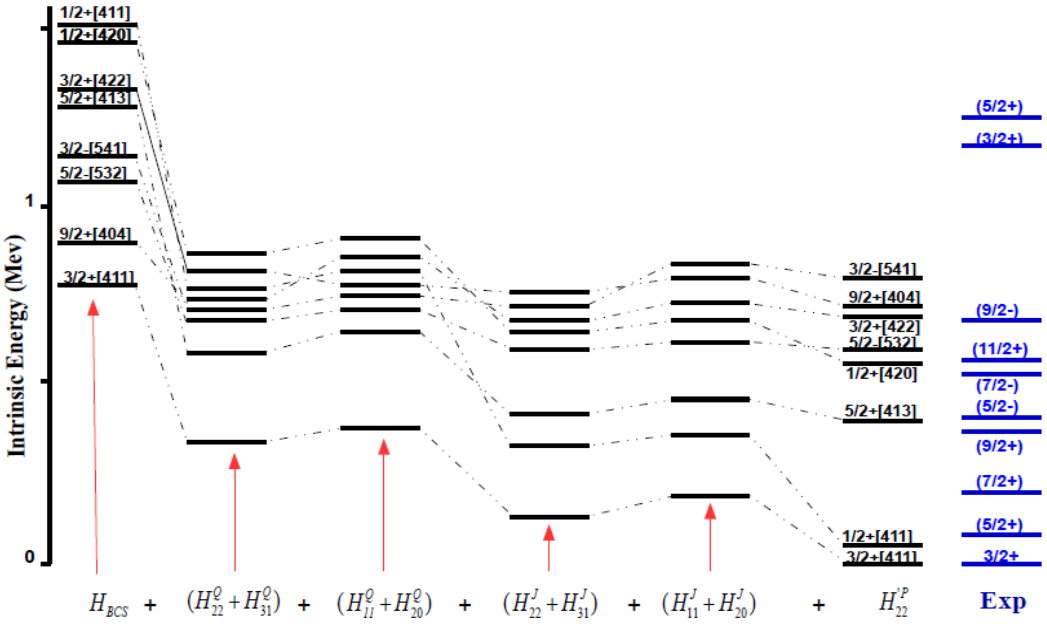

Fig.1: Energy evolution of intrinsic states in ^{99}Sr caused by including successive interaction terms of quadrupole and recoil forces to the initial pairing interaction

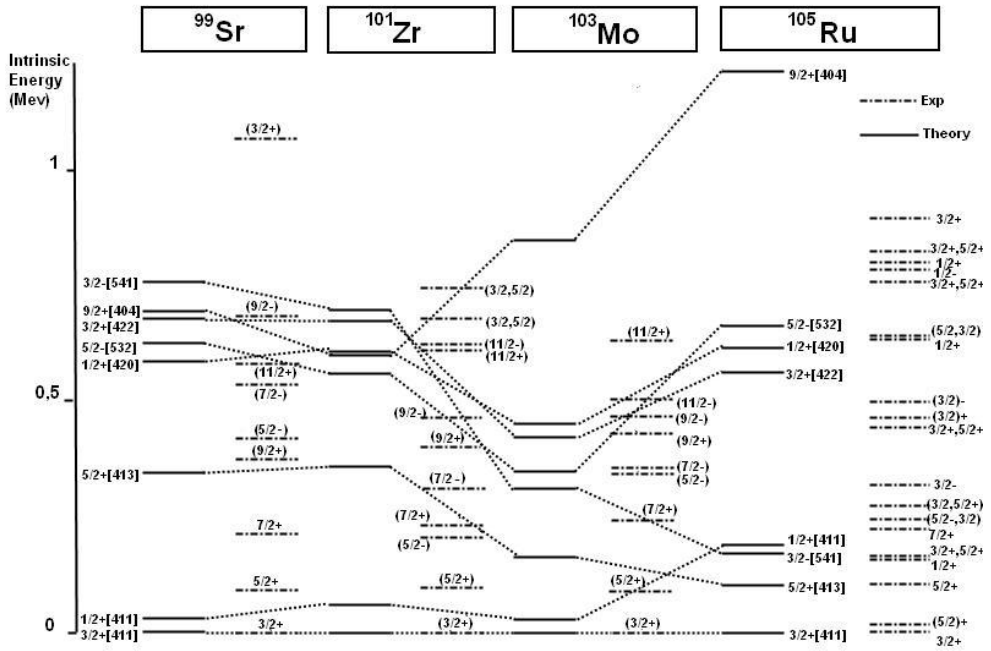

Fig.2: Systematic of the low lying states in N=61 isotones ^{99}Sr, ^{101}Zr,^{103}Mo and ^{105}Ru

Here, we can see that by adding quadrupole and recoil forces to pairing interaction a new arrangement of intrinsic energies is obtained. Thus, for the quadrupole force we notice that both two-body and one-body terms exhibit important interaction for positive parity states than negative parity ones. The influence is so high as states have a small spin. This situation changes with the recoil force which preferentially influences the negative parity states. The effect due to the last term H_{22}^{P} in (10) is in general small. The results of calculations obtained by considering all terms of the intrinsic Hamiltonian are given in table 4.

The low-lying intrinsic states in ^{99}Sr with a calculated energy up to 1,5Mev are presented. Only components C_v or D_v which contribution to the normalization of wave function is more than 1% are shown. The calculated energy position reproduces the observed positive parity bandhead. Also, an important contribution from the quasiparticle-phonon coupling is established for the configuration of positive parity wave functions. However, for the negative parity wave function, the configuration indicates a large component related to only a one-quasiparticle excitation. One can then consider the negative parity intrinsic states in ^{99}Sr as been a pure one-quasiparticle excitation without any contribution from the vibrational excitation mode. The construction and diagonalization of the total Hamiltonian matrix are performed by using the basis function (5). The energies and wave functions of rotational bands based upon the dominant intrinsic states are determined for each value of the total angular momentum and parity.

In Fig. 2, the isotonic chain for N = 61 (^{99}Sr, ^{101}Zr, ^{103}Mo and ^{105}Ru) is reproduced by our QPRM calculations, in respect to deformation parameters given by Moller [17], and compared to the existing experimental data. The ground state corresponds to 3/2+(411) states both experimentally and theoretically is present, the odd neutron determines the spin and parity of the ground state. First one realizes the observed experimental correspondence between the spins and parities of isotones within Sr, Zr, Mo and Ru nuclei. It, therefore, holds that the positive parity states are very sensitive to the quadrupole interaction and recoil force; whereas the negative parity states were influenced only by the terms of the one-body of recoil force.

Then we can deduce that the nuclear shape is determined by a competition between a quadrupole force and a pairing force. The quadrupole force tends to deform the nucleus while the spherical shape is stabilized by the pairing force. With only a small number of nucleons outside a closed shell, pairing dominates, and the nucleus remains spherical. When more nucleons are added, the relative strength of the quadrupole force increases and at a certain point a transition to a deformed shape takes place. Therefore deduces from the vibration is dominant over rotation for nuclei with few valence nuclei outside the spherical core. Pure rotational spectra are only observed for nuclei with a large number of valence nucleons, which can correlate to form stable deformation. The general case is a mixture of all three, but as a first approximation they can be separated, and treated independently. We can deduce that nuclear structure of rich-neutron nuclei in the transition region with A ~ 100 is very complex. To better interpret the experimental data, we must consider models that are based on the unification of all modes of excitation.

Conclusion

In this contribution, some recent results obtained within a fully microscopic model beyond mean-field will be reviewed. Our model is based on the coupling between quasiparticle and collective degrees of freedom. Moreover, as vibration mixing at low-lying excitations is also expected, some calculations based upon the quasiparticle-phonon coupling plus rotor method (QPRM) have been carried out for isotopic chain of odd-A Sr, Zr, Mo and Ru isotones. It is now well established that the three shapes coexist in neutron-rich nuclei in the transitional region with A~100. Our theoretical interpretation of these collective bands is based on coupling between axially rotational motion and vibration instead of triaxial deformed nuclei. We have shown the importance of band-mixing effect due to Coriolis force. We remark also that the band head is determined by a competition between a quadrupole force and a pairing force, the quadrupole force tends to deform the nucleus while the spherical shape is stabilized by the pairing force. When more nucleons are added to the spherical shape (closed shell), the relative strength of the quadrupole force increases and at a certain point the transition to the deformed shape takes place. This competition plays a very important role in the shape coexistence. However, we are aware of the challenge of reproducing in detail the observed spectroscopic properties in the particular mass region considered in the present study.

References

[1]. J.A.Pinston,W.urban,Ch.Droste,J.Genevey,T.Rzaca-Urban (October 2006).
[2]. G. Georgiev *et al*, CERN- INTC- 2009- 019/ INTC- P- 266 (2009).
[3]. H.B. Ding *et al* , phy. review C74,054301 (2006).
[4]. R. Orlandi *et al*, Physical Review C73, 054310 (2006).
[5]. H. Hua *et al* Physical Review C 69,014317 (2004).
[6]. V.G. Soloviev, Theory of Complex Nuclei, Pergamon Press, Oxford, England, 1976.
[7]. O. Jdair, J. Inchaouh, M. K. Jammari, H. Chakir, Vol.3.N°2.March, 2011, Part IV (International Journal of Academic Research).
[8]. J.Inchaouh , K.Jammari, O.Jdair, A. Khouaja, M.L.Bouhssa, H. Chakir and A. Morsad. Physical Review C 2013; 88: 064301(12).
[9]. P. Ring et P. Schuck, the nuclear Many-body Problem (Springer, New York 1980)
[10]. Nuclear Data Sheets 112 (2011) 275–446

[11]. Nuclear Data Sheets 83, 1 (1998) Article No. DS980001
[12]. Nuclear Data Sheets 110 (2009) 2081–2256
[13]. Nuclear Data Sheets 105 (2005) 775–958
[14]. J. M. Eisenberg and W. Greiner; Nuclear Models, Vol. 1 (Elsevier, New-York, 1970)
[15]. J. P. Boisson and R. Piepenbring; Nucl. Phys. A168 (1971) 385
[16]. A. Bohr and B. R. Mottelson, Nuclear Structure Vol. 2, Benjamin (1975)
[17]. P. Moller et al, Atomic data and Nuclear Data tables, Vol.59, N°. 2 (1995)185
[18]. R. A. Meyer *et al* Nucl. Phys. A439, 510 (1985)
[19]. P. Moller, J. R. Nix, Nucl. Phys. A536 (1992)20
[20]. Nuclear Data Sheets 84,565 (1998)
[21]. Nuclear Data Sheets109 (2008)
[22]. Nuclear Data Sheets 110 (2009) 1745–1915
[23]. Nuclear Data Sheets 108 (2007) 2035–2172
[24]. L. Grodzins, Phys.Lett.2 (1962) 88
[25]. F.S.Stephens *et al*, Phys. Rev. Lett.29 (1972) 438
[26]. C. M. Petrache, Y. Sun, D. Buzzacco, S. Lunardi, C. Rossi Alvarez, R. Venturelli, D. De Acuña, G. Maron, M. N. Rao Z. Podolyak, at J. R. B. Oliveira ; Phys. Rev. C53 (1996) R2581